Neuro-Oncology

Neuro-Oncology 16(1), 50–61, 2014
doi:10.1093/neuonc/not157
Advance Access date 4 December 2013

MDA-9/syntenin is a key regulator of glioma pathogenesis

Timothy P. Kegelman, Swadesh K. Das, Bin Hu, Manny D. Bacolod, Christine E. Fuller, Mitchell E. Menezes, Luni Emdad, Santanu Dasgupta, Albert S. Baldwin, Jeffrey N. Bruce, Paul Dent, Maurizio Pellecchia, Devanand Sarkar, and Paul B. Fisher

Department of Human and Molecular Genetics, Virginia Commonwealth University, School of Medicine, Richmond, Virginia (T.P.K., S.K.D., B.H., M.D.B., M.E.M., L.E., S.D., D.S., P.B.F.); VCU Institute of Molecular Medicine, Virginia Commonwealth University, School of Medicine, Richmond, VA (S.K.D., M.D.B., L.E., S.D., P.D., D.S., P.B.F.); Department of Pathology, Virginia Commonwealth University, School of Medicine, Richmond, Virginia (C.E.F.); VCU Massey Cancer Center, Virginia Commonwealth University, School of Medicine, Richmond, Virginia (S.K.D., M.D.B., L.E., S.D., P.D., D.S., P.B.F.); Department of Biology, University of North Carolina, Chapel Hill, North Carolina (A.S.B.); Department of Neurosurgery, Columbia University, College of Physicians and Surgeons, New York, New York (J.N.B.); Department of Neurosurgery, Virginia Commonwealth University, School of Medicine, Richmond, Virginia (P.D.); Sanford-Burnham Medical Research Institute, La Jolla, California (M.P.)

Corresponding author: Paul B. Fisher, MPh, PhD, Professor and Chairman, Department of Human and Molecular Genetics, Director, VCU Institute of Molecular Medicine, VCU Massey Cancer Center, Virginia Commonwealth University, School of Medicine, 1101 East Marshall Street, Sanger Hall Building, Room 11–015, Richmond, VA 23298-0033 (pbfisher@vcu.edu).

Background. The extraordinary invasiveness of human glioblastoma multiforme (GBM) contributes to treatment failure and the grim prognosis of patients diagnosed with this tumor. Consequently, it is imperative to define further the cellular mechanisms that control GBM invasion and identify promising novel therapeutic targets. Melanoma differentiation associated gene–9 (MDA-9/syntenin) is a highly conserved PDZ domain–containing scaffolding protein that promotes invasion and metastasis in vitro and in vivo in human melanoma models. To determine whether MDA-9/syntenin is a relevant target in GBM, we investigated its expression in tumor samples and involvement in GBM invasion and angiogenesis.

Materials. We assessed MDA-9/syntenin levels in available databases, patient tumor samples, and human-derived cell lines. Through gain-of-function and loss-of-function studies, we analyzed changes in invasion, angiogenesis, and signaling in vitro. We used orthotopic xenografts with GBM6 cells to demonstrate the role of MDA-9/syntenin in GBM pathogenesis in vivo.

Results. MDA-9/syntenin expression in high-grade astrocytomas is significantly higher than normal tissue counterparts. Forced overexpression of MDA-9/syntenin enhanced Matrigel invasion, while knockdown inhibited invasion, migration, and anchorage-independent growth in soft agar. Moreover, overexpression of MDA-9/syntenin increased activation of c-Src, p38 mitogen-activated protein kinase, and nuclear factor kappa-B, leading to elevated expression of matrix metalloproteinase 2 and secretion of interleukin-8 with corresponding changes observed upon knockdown. GBM6 cells that stably express small hairpin RNA for MDA-9/syntenin formed smaller tumors and had a less invasive phenotype in vivo.

Conclusions. Our findings indicate that MDA-9/syntenin is a novel and important mediator of invasion in GBM and a key regulator of pathogenesis, and we identify it as a potential target for anti-invasive treatment in human astrocytoma.

Keywords: MDA-9/syntenin, GBM, glioma, invasion, intracranial injection.

In the United States, an estimated 69 720 new cases of primary CNS tumors will be diagnosed in 2013.[1] Gliomas, named for the normal glial cell to which they bear the closest resemblance, encompass a wide histology of tumors and account for 80% of malignant primary CNS neoplasms. Over 75% of all gliomas are astrocytomas, which are composed of neoplastic astrocytes and range in grade from low-grade pilocytic astrocytoma (grade I) to high-grade tumors (grade IV, glioblastoma multiforme [GBM]).[2] GBM is a notoriously aggressive, proliferative, and invasive tumor that, despite recent advances in radiation and chemotherapies, has a 5-year survival rate of $<5\%$.[1] Furthermore, surgical resection to remove all of the tumor is difficult or impossible because of the vital nature of the surrounding tissue and is not curative due to the ability of single GBM cells to migrate from the primary tumor mass.[3]

While all higher-grade astrocytic tumors demonstrate diffuse infiltration, GBM is particularly adept at invading the brain

Received 29 October 2012; accepted 26 August 2013

parenchyma.[4] Rapid growth along myelinated portions leads to supratentorial bilateral extension of these tumors, notably along the fornices toward the temporal lobes and across the corpus callosum, leading to a "butterfly glioma" pattern. In addition to tracking along myelinated structures, another avenue of invasion is observed within and along perivascular spaces.[5] A detailed understanding of the involved and layered regulation of glioma invasion is only beginning to form.[4] Nonetheless, crucial differences in how normal glial migration differs from glioma cell migration have yet to be uncovered.[6]

To successfully invade the surrounding tissue, a glioma cell must detach from the primary mass, adhere to and degrade the extracellular matrix (ECM), and engage processes of cell motility and contractility.[4] After breaking from the primary tumor, glioma cells adhere to the ECM most often through interactions utilizing integrins, transmembrane glycoprotein heterodimers. Integrins associate with an assortment of ECM proteins, including fibronectin, vitronectin, and fibrinogen, and increased expression of integrins can lead to increased cell motility in glioma cells.[6] Next, invading cells use matrix metalloproteinases (MMPs), including MMP2 and MMP9, to degrade ECM, which can be regulated by the transcription factor nuclear factor kappa-light-chain-enhancer of activated B cells (NF-κB).[6] Once a path is cleared, glioma cell locomotion relies on the function of actin, responsible for driving the leading processes of migrating cells, and the dynamics of myosin II, a major generator of contractile force.[7]

Melanoma differentiation associated gene-9 (*mda-9*),[8] also known as syntenin,[9] is an intriguing protein with involvement in a plethora of cellular functions.[10–13] In addition to roles in cell-cell and cell-matrix adhesion, MDA-9/syntenin is an integral element in signal transduction from the cell's surface to the interior; levels of MDA-9/syntenin are detectable in all human fetal and adult tissues and the gene has been shown to be highly homologous across species.[13] *mda-9*/syntenin was first identified as a biphasic-expressing gene through subtraction hybridization comparing human melanoma cells in unaltered and terminally differentiated states, suggesting a potential role in melanoma pathogenesis.[8,14] This view was confirmed by later studies that revealed the influence of MDA-9/syntenin as a positive regulator of the progression and metastatic potential of human melanoma through interactions with c-Src.[15–18] By facilitating active focal adhesion kinase (FAK)/c-Src complexes, MDA-9/syntenin amplifies signaling through a p38 mitogen-activated protein kinase (MAPK)–dependent pathway, ultimately activating NF-κB and leading to upregulation of MMP activity. Furthermore, forced expression of MDA-9/syntenin results in increased migration by nonmetastatic cancer cells, and manifests an increasingly polarized distribution of F-actin and greater pseudopodia formation. In addition to melanoma, MDA-9/syntenin was found at increased levels in multiple breast and gastric cancer cell lines and in a single genetically uncharacterized human glioma cell line, contributing to cell migration.[19,20]

In addition to established roles in human melanoma, MDA-9/syntenin has been shown to be important in gastrulation and nervous system development. In zebrafish, MDA-9/syntenin was essential for epiboly and implicated in actin cytoskeleton rearrangement.[21] In investigations of processes of neural development, MDA-9/syntenin was shown to bind neurofascin, SynCAM, and neurexin, cell adhesion molecules involved in axonal growth and proper formation of synaptic structures (reviewed by Das et al[12]). One of the earliest genes expressed during neuronal differentiation, serine/threonine kinase Unc51.1, uses MDA-9/syntenin as a scaffold, as does Rab5 GTPase, a regulator of endocytosis and membrane organization during axon outgrowth.[22]

The current studies demonstrate that MDA-9/syntenin expression is increased in multiple neuroepithelial tumors of the CNS. Focusing on glioma cell lines, we demonstrate that expression of MDA-9/syntenin is elevated compared with controls and correlates with increasing tumor grade in patient samples. Additionally, we characterize MDA-9/syntenin as a driver of glioma motility and invasion, acting through a c-Src–dependent pathway leading to the activation of NF-κB.

Materials and Methods

Construction of Plasmids, Adenoviruses, and Stable Cell Lines

Small hairpin (sh)RNA for *mda-9*/syntenin (sh*mda-9*/syntenin) has been constructed with pSilencer hygro expression vectors according to the manufacturer's protocol (Ambion). Specific hairpin small interfering (si)RNA oligonucleotides (sense 5′-GATCCGCGGATGGCACCAAGCATTTTCAAGAGAAATG CTTGGTGCCATCCGCTTTTTTGGAAA-3′ and antisense 5′-AGCTTTTCCAAAAAA GCGGATGGCACCAAGCATTTCTCTTGAAAATGCTTGGTGCCATCCGCG-3′) were annealed and ligated to pSilencer vector by T4 DNA ligase. The genomic sequence of *mda-9*/syntenin was amplified by PCR using genomic DNA as template and primers, sense: 5′-CTGCAAAAATGTCTCTCTATCC-3′ and antisense: 5′-GGTGCCGTGAATTTTAAACCTCAG-3′. The PCR product was cloned into pREP4 expression vectors, from where it was digested and released with *Xho* and *Bam*H1 and subcloned into the pcDNA3.1 (+hygro) (Invitrogen). The DNA fragment (702 bp) containing the U6 promoter followed by oligonucleotide encoding shRNA designed for the *mda-9*/syntenin gene was isolated from *Eae*I-digested pSilencer–sh*mda-9* plasmid and then cloned into the *Not*I site of pShuttle (pSh) plasmid generating psh*mda-9*-shuttle vector. To construct the shuttle vector pShCMV–MDA-9, *Bam*HI and *Eco*RV DNA fragment (990 bp) containing the *mda-9*/syntenin gene was isolated from plasmid p0tg-CMV–MDA-9 22 and cloned between *Bgl*II and *Eco*RV sites downstream of the cytomegalovirus (CMV) promoter in plasmid pSh-CMV. The shuttle plasmids were recombined with genomic DNA of Ad.5/3.*Luc1* vector as we previously described[23] to derive plasmids pAd.5/3–sh*mda-9* or pAd.5/3–*mda*-9. The resultant plasmids were cleaved with PacI to release the recombinant adenovirus genomes and then transfected to human embryonic kidney (HEK)–293 cells to rescue the corresponding Ad.5/3-based vectors. The rescued viruses were upscaled using HEK-293 cells and purified by cesium chloride double ultracentrifugation using standard protocol, and the titers of infectious viral particles were determined by plaque assay using HEK-293 cells as described.[24]

Alternate siRNA sequences were obtained through Qiagen with the following sequences: 5′-TTGACTCTTAAGATTATGTAA-3′ (si*mda-9* #3) and 5′-TGGGATGGTCTTAGAATATTT-3′ (si*mda*-9 #4). Ad.5/3 sh*mda-9* resistant *mda-9*/syntenin was constructed using the following primer sequences: forward 5′-GCCTGCTTTTATCTTTGAACATATTATTAAGCGAATGAAGCCTAGTATA ATGAAAAGCCTAATGGACCACACCATTCCTGAG-3′ and reverse: 3′-CGGACGA AAATAGAAACTTGTATAATAATTCGCTTACTTCGGATCATATTACTTTTCGGATTACCT GGTGTGGTAAGGACTC-5′.

Cell Lines, Cell Culture, and Human Tissue Samples

Human malignant glioma cells U87, U251, and T98G as well as grade III astrocytoma lines Sw1088 and Sw1783 were purchased from the American Type Culture Collection. Human primary GBM6 cells were described previously and were provided by Dr C. David James (University of California, San Francisco).[25] Cells were cultured in Dulbecco's modified Eagle's medium (DMEM) + F12 supplemented with 10% fetal calf serum in a

37°C incubator supplemented with 5% CO_2. Primary human fetal astrocytes (PHFAs) were obtained from preterm abortions as previously described with institutional review board approval, and human telomerase reverse transcriptase (h-TERT)–immortalized (IM) PHFAs were produced and cultured as described.[26] All cells were routinely screened for mycoplasmal contamination. Specimens of human primary brain tumors were collected from subjects who underwent surgical removal of their brain tumors at the Department of Neurosurgery, New York Presbyterian Hospital, Columbia University. All subjects were informed of the nature and requirements of the study and provided written consent to donate their tissues for research purposes. Tumor specimens of all histological types and grades of primary brain tumors were collected, snap frozen, and stored in the tumor bank following the protocol approved by an institutional review board.

Preparation of Whole-cell Lysates and Western Blotting Analysis

Preparation of whole-cell lysates and western blotting analysis were done as described.[27] For densitometric evaluation, X-ray films were scanned and analyzed with ImageJ software (National Institutes of Health [NIH]).

Antibodies and Reagents

Antibodies against IκBα, phospho-IκBα (Ser32/36), p38MAPK, phospho-p38MAPK (Thr180/Tyr182), Src, and phospho-Src (Tyr 416) were obtained from Cell Signaling. MMP2, β-actin, and α-tubulin were obtained from Abcam, and MDA-9/syntenin from Abnova. MDA-9/syntenin used for immunohistochemistry (HPA023840) was purchased from Sigma-Aldrich, as was fibronectin, and SB203580 was purchased from Calbiochem. Inhibitor of kappa B kinase (IKK) inhibitor was kindly provided by Dr Albert S. Baldwin, Jr (University of North Carolina, Chapel Hill).

Immunohistochemistry

A portion of the frozen tumor specimen was fixed in phosphate-buffered formalin and preserved as paraffin sections following standard procedure for the maintenance of histological structure. Paraffin-embedded sections were dewaxed and rehydrated through incubations in xylene and a gradient series of alcohol. Antigen retrieval was processed in 10 mM citric acid (pH 6.0) with microwave treatment for 20 min. Endogenous hydrogen peroxidase was quenched with 3% H_2O_2 for 20 min. After blocking nonspecific binding sites with 5% normal sera, the sections were incubated overnight with antibody. The sections were incubated with appropriate biotinylated secondary antibody and subsequently with avidin-biotin-peroxidase complex (Vector Elite, Vector Laboratories). Colorimetric reactions were developed by incubation in diaminobenzidine substrate (0.02% diaminobenzidine, 0.005% hydrogen peroxide) and counterstained with 10% Harris' hematoxylin. Hematoxylin and eosin staining was conducted following a standard protocol.[17] The images were analyzed under the Olympus BX41 microscope system equipped with a DP25 digital camera and software. Tissue microarray CNS2081 was purchased from US Biomax.

Upon analyzing MDA-9/syntenin staining of normal brain and lymph node tissue (positive control), Dr Christine Fuller scored the CNS2081 tissue microarray on a scale of 0–3. Average scores for each of the 104 cores were used to calculate mean scores for each tissue group. Scores were compared with cancer adjacent tissue and normal brain tissue using Student's *t*-test.

Invasion and Migration Assays

Invasion was measured using 24-well BioCoat cell culture inserts (BD Biosciences) with an 8-μm-porosity polyethylene terephthalate membrane coated with Matrigel Basement Membrane Matrix (100 $\mu g/cm^2$). Briefly, the Matrigel was allowed to rehydrate for 2 h at 37C by adding warm, serum-free DMEM. The wells of the lower chamber were filled with medium containing 5% fetal bovine serum. Cells (5×10^4) were seeded in the upper compartment (6.25-mm membrane size) in serum-free medium. The invasion assay was done at 37°C in a 5% CO_2 humidified incubator for 18 h. At the end of the invasion assay, filters were removed, fixed, and stained with the Diff-Quick Staining kit (IMEB). Cells remaining on the upper surface of the filters were removed by wiping with a cotton swab, and invasion was determined by counting the cells that migrated to the lower side of the filter using at least 5 fields per insert at 100× magnification. Wound healing scratch motility assays were done as described previously.[17] Data from triplicate experiments were expressed as mean ± 95% confidence interval (CI).

Anchorage-independent Growth Assays in Soft Agar

Anchorage-independent growth assays were performed by seeding 5×10^4 cells in the CytoSelect Cell Transformation Assay (Cell Biolabs) in 24-well plates according to the manufacturer's instructions. Colonies were counted 12 days after seeding and analyzed using ImageJ colony counter (NIH). The data from triplicate wells were expressed as mean ± 95% CI.

Preparation of Conditioned Media

Conditioned media were harvested from an overnight culture of plated cells in serum-free DMEM + F12 media, filtered with 0.2 μM filters and further concentrated 10-fold on an Amicon Ultra centrifugal filter –3 K (Millipore).

Virus Infections and Reporter Assays

Viral infection conditions and protocols were performed as delineated previously.[17] Luciferase reporter assays were performed using 2×10^5 cells infected with either Ad.5/3-*vec* or Ad.5/3–*mda-9*. Twenty-four hours post-infection, cells were transfected with an NF-κB–responsive luciferase reporter construct with Lipofectamine 2000 as described.[16,17] Forty-eight hours after transfection, cells were trypsinized and plated on fibronectin-coated surfaces (10 μg/mL) in serum-free medium for 1 h. Cell lysates were harvested and luciferase activity was measured using a Dual-Luciferase Reporter Assay system (Promega) according to the manufacturer's instructions. Luciferase activity was normalized by Renilla activity, and data represent the average of triplicates ± SD.

Human Angiogenesis Arrays and Chicken Chorioallantoic Membrane Assays

Using conditioned media, equal amounts of protein (500 μg) in 100-μL samples were assayed using human angiogenesis antibody arrays (R&D Biosystems) and processed according to the manufacturer's instructions. Chicken chorioallantoic membrane (CAM) assays were performed using 9-day-old chick embryos; cells were seeded on the CAM surface according to established protocols.[28] One week after inoculation, the neovasculature was examined and photographed.

Xenograft Studies in Athymic Nude Mice

Subcutaneous xenografts were established in the flanks of athymic nude mice (4- to 5-wk-old female mice, from Charles River) using 1×10^5 cells and followed for 3 weeks. Tumor volume was measured 3 times weekly with a caliper and calculated using the following formula: $\pi/6 \times$ larger diameter $\times$ (smaller diameter).[2] Postsacrifice, the tumors were resected, weighed, and preserved for immunohistochemical staining.

Intracranial Implant of GBM6 Cells in Nude Mice

Athymic female NCr-nu/nu mice (National Cancer Institute–Frederick) weighing ~20 g were used for this study. Mice were maintained under pathogen-free conditions in facilities approved by the American Association

for Accreditation of Laboratory Animal Care and in accordance with current regulations and standards of the US Department of Agriculture, the US Department of Health and Human Services, and the NIH. At least 10 mice per group were utilized. Mice were anesthetized through i.p. administration of ketamine (40 mg/kg) and xylazine (3 mg/kg) and immobilized in a stereotactic frame (Stoelting). A 24-gauge needle attached to a Hamilton syringe was inserted into the right basal ganglia to a depth of 3.5 mm and then withdrawn 0.5 mm to make space for tumor cell accumulation. The entry point at the skull was 2 mm lateral and 1 mm dorsal to the bregma. Intracerebral injections of 1.5×10^4 cells in 2 μL per mouse were completed over 10 min using an automated injector (Stoelting). The skull opening was enclosed with sterile bone wax, and the skin incision was closed using sterile surgical staples.

Database Mining

We surveyed 2 publicly available databases: (i) The Cancer Genome Atlas (TCGA) that combined low- grade glioma (LGG) and GBM datasets (https://tcga-data.nci.nih.gov/tcga/), generated using Illumina HiSeq 2000 RNA Sequencing, and (ii) the National Center for Biotechnology Information Gene Expression Omnibus (NCBI-GEO) dataset GSE4290,[29] derived by using the Affymetrix HG U133 Plus 2 platform. The datasets were obtained through the NCBI-GEO and the University of California, Santa Cruz Cancer Genomics Browser[30] websites, respectively, and data were analyzed using the Gene-E (Broad Institute) and JMP Pro 10 (SAS) analytical/statistical programs.

Statistical Analysis

The data are reported as the mean ± SD of the values from 3 independent determinations, and significance analysis was performed using the Student's *t*-test in comparison with corresponding controls. $P < .05$ was considered statistically significant. Survival curves were analyzed using Cox proportional hazards survival regression (http://statpages.org/prophaz.html).

Results

Elevated MDA-9/syntenin Expression Is Common in Neuroepithelial Tumors of the CNS and Correlates With Astrocytoma Tumor Grade

Given the increased expression of MDA-9/syntenin observed in human melanoma, we asked whether similar trends were evident

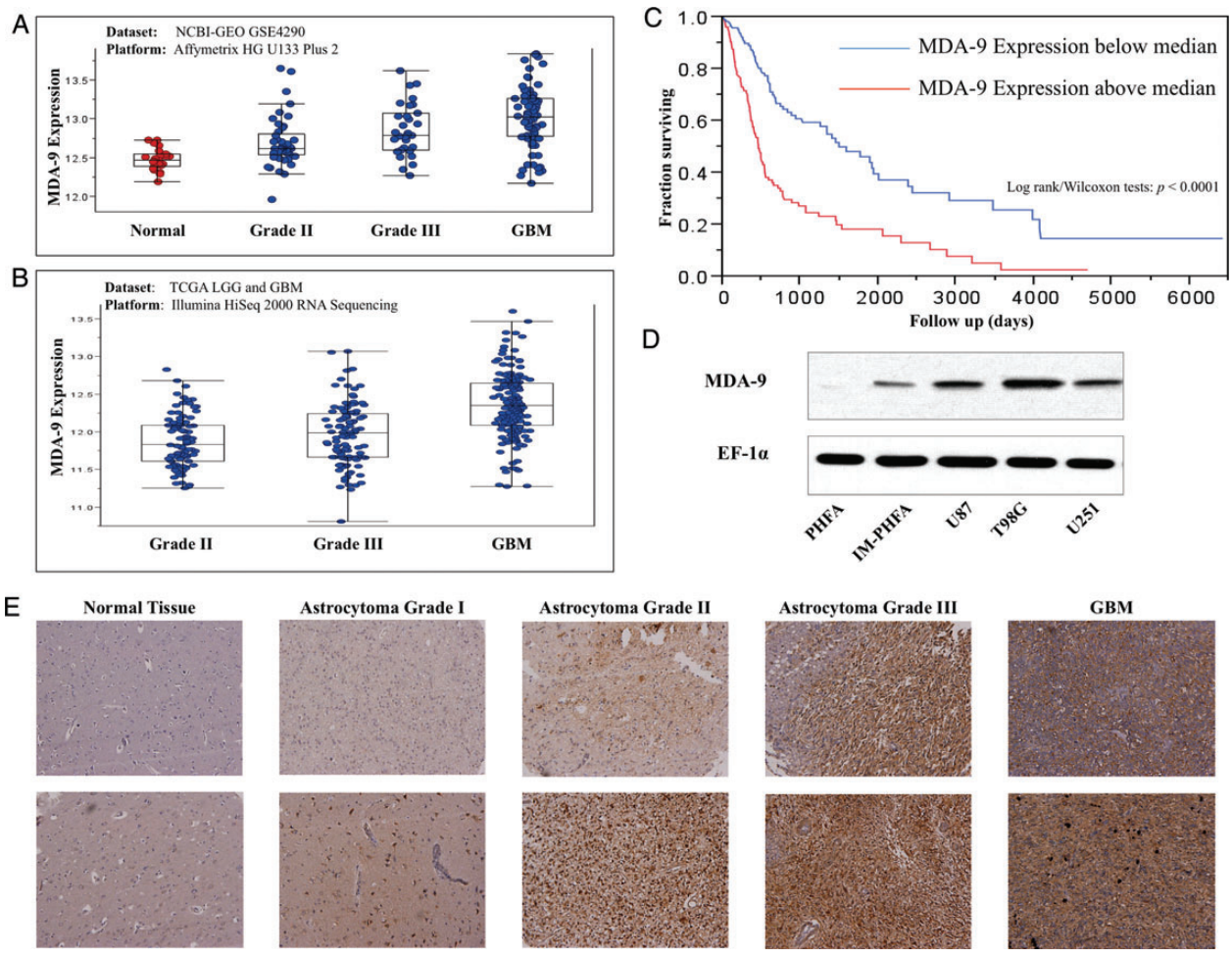

Fig. 1. *mda-9*/syntenin is overexpressed in glioma clinical samples and cell lines. (A) *mda-9*/syntenin expression in glioma tumor grade compared with normal tissue using the NCBI-GEO GSE4290 dataset. (B) *mda-9*/syntenin expression in varying grades of glioma tumors using the TCGA LGG and GBM dataset. (C) Kaplan–Meier survival plot comparing survival time according to *mda-9*/syntenin expression. High expression: *mda-9*/syntenin levels above median. Low expression: *mda-9*/syntenin levels below median. (D) *mda-9*/syntenin expression in various cell lines. (E) Representative images of *mda-9*/syntenin expression in normal and tumor samples. ** $P < .05$.

in primary brain tumors. To answer this question, we analyzed TCGA combining LGG and GBM datasets and the NCBI-GEO dataset.[29] As both datasets indicate (Fig. 1A and B), the *mda*-9/syntenin transcription level, on average, increases as tumor grade progresses (ANOVA test, $P < .0001$ in both datasets). In the GSE4290 dataset, nontumor cases were obtained from epilepsy patients. As of this writing, reference (normal) cases are not included in the LGG and GBM datasets of TCGA.

Increased expression of *mda-9*/syntenin appears to be a clinically important phenomenon, as shown by analysis of TCGA patient survival segregated by expression (Fig. 1C). Patients with gliomas expressing above median levels of *mda-9*/syntenin show a marked decrease in survival compared with those with below median *mda-9*/syntenin (Kaplan–Meier survival analysis, $P < .0001$ in both log-rank and Wilcoxon statistical tests).

To validate these observations from genomic datasets, we analyzed a tissue microarray consisting of 104 cores, including tumor, cancer adjacent normal, and normal tissues. In these samples, specimens were classified according to World Health Organization grades of brain tumors,[2] and strength of MDA-9/syntenin staining was scored (Table 1). We found that astrocytomas of all grades had significantly higher MDA-9/syntenin expression than normal tissue counterparts (Fig. 1E). We determined that in human astrocytomas taken together, similar to the pattern observed in human melanomas, elevated MDA-9/syntenin was more common in high-grade tumors. Protein expression of MDA-9/syntenin was verified by western blotting in 46 specimens from surgically removed primary brain tumors. When compared with samples obtained from normal brain tissue, which expectedly showed low but detectable levels, tumor tissue showed high expression of MDA-9/syntenin more frequently (Supplementary Figs. 1, 2). Cell lines used in vitro were then analyzed for MDA-9/syntenin expression level. Barely detectable levels were observed in PHFAs, and slightly higher levels were found in h-TERT IM-PHFA cells, while robust expression was seen in GBM lines U87MG, T98G, and U251 (Fig. 1D).

Table 1. Tumor sections from listed types were scored (0–3) for MDA-9/syntenin expression

	Average Score	*n* Samples	*P* vs	
			CAT	NT
Astrocytoma grade I	2.67 ± 0.52	6	.007	.077
Astrocytoma grade II	2.82 ± 0.40	11	.0002	.007
Astrocytoma grade III	3.00 ± 0.00	7	.001	.007
GBM	2.75 ± 0.46	8	.001	.028
Oligodendroglioma	3.00 ± 0.00	5	.003	.023
Malignant oligodendroglioma	2.83 ± 0.29	3	.028	.120
Ependymoma	1.33 ± 0.58	3	.608	.491
Malignant ependymoma	2.80 ± 0.45	5	.008	.061
Medulloblastoma	2.80 ± 0.42	10	.0003	.011
CAT	0.94 ± 1.21	8	1.000	.165
NT	1.79 ± 0.99	7	.165	1.000

Right columns compare average tumor section scores with average scores for cancer-adjacent normal tissue (CAT) or normal brain tissue (NT).

MDA-9/syntenin Protein Level Correlates With Changes in the Invasive Ability of Astrocytoma Cells

Next, we determined whether manipulating MDA-9/syntenin expression could lead to changes in invasion in vitro. Accordingly, MDA-9/syntenin expression was reduced in GBM cell lines T98G and U87MG using an adenovirus expressing shRNA targeted to *mda-9*/syntenin. Cells treated with Ad.5/3–sh*mda-9* had approximately a 5-fold decrease in invasive ability compared with vector (Ad.5/3-con sh)-treated cells ($P < .001$; Fig. 2A). Conversely, MDA-9/syntenin was overexpressed using adenovirus (Ad.5/3–*mda-9*) in 3 cell lines that normally express low levels: IM-PHFA, Sw1783, and GBM5. When compared with cells infected with vector alone (Ad.5/3-*vec*), cells that overexpressed MDA-9/syntenin after Ad.5/3–CMV–*mda-9* (Ad.5/3–*mda-9*) treatment invaded at significantly higher rates, with 2-, 3-, and 5-fold increases (IM-PHFA, Sw1783, GBM5), respectively, in invasion ($P < .001$; Fig. 2B). To account for the possibility of off-target effects, we used multiple alternative siRNA sequences for knockdown experiments and an *mda-9*/syntenin construct designed to be resistant to Ad.5/3–sh*mda-9*. Similar results were observed when using alternative siRNA sequences. Protein levels and invasion were reduced at levels equivalent to those observed using Ad.5/3–sh*mda-9* (Supplementary Fig. 3). Additionally, a plasmid construct with sequences mutated to be resistant to the targeting of our adenoviral vector rescued invasiveness in the presence of Ad.5/3–sh*mda-9* (Supplementary Fig. 4).

MDA-9/syntenin Signaling Is c-Src Dependent and Activates NF-κB Through the p38MAPK Pathway

To determine the mechanism by which MDA-9/syntenin provokes changes in downstream signaling, we analyzed protein levels in astrocytoma cells after MDA-9/syntenin manipulation (Fig. 3A). In previous studies, c-Src was found to be an important interacting partner and effector of MDA-9/syntenin signaling, contributing to a metastatic phenotype in human melanoma.[15–18] Indeed, overexpression of MDA-9/syntenin in Sw1783 and GBM5 cells leads to increased levels of activated Src. Conversely, reducing MDA-9/syntenin in T98G and U87MG cells lowers phosphorylated Src levels. Initiation of c-Src signaling can lead to activation of the p38MAPK pathway and ultimately to NF-κB activation and the transcription of cellular genes involved in invasion. Phosphorylated p38MAPK was increased upon MDA-9/syntenin overexpression in Sw1783 and GBM5 cells. A decrease in activated p38MAPK was also observed after knockdown of MDA-9/syntenin. The phosphorylation of IκBα, which normally maintains NF-κB in an inactive state in the cytoplasm, targets it for degradation, leaving NF-κB free to translocate into the nucleus. When MDA-9/syntenin is overexpressed, there is an increase in phosphorylated IκBα and a concomitant increase in MMP2, a known target of NF-κB. Likewise, infection with Ad.5/3–sh*mda-9* reduced phosphorylated IκBα and MMP2.

As in previous studies performed in human melanoma,[16] we found that MDA-9/syntenin bound to Src in GBM cells by immunoprecipitation (Supplementary Fig. 5). To determine whether the increase in invasion correlating with MDA-9/syntenin overexpression was dependent on c-Src, we transfected plasmids encoding wild-type or dead kinase Src, which acts as a dominant negative protein, along with a control plasmid or *mda-9*/syntenin into

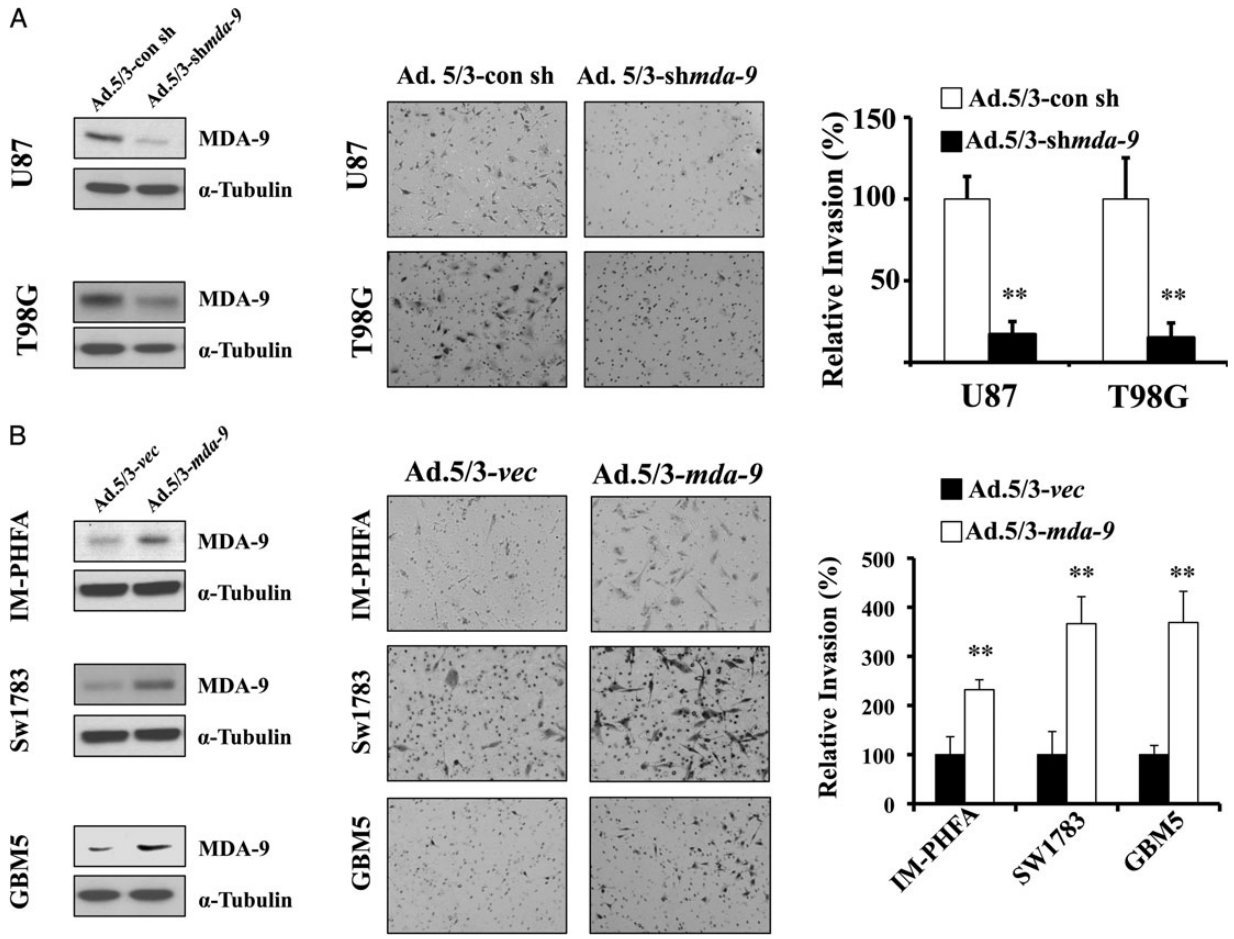

Fig. 2. MDA-9/syntenin regulates astrocytoma invasion. (A) Knockdown of MDA-9/syntenin leads to decreases in invasion. *(Left)* Protein expression of MDA-9/syntenin after viral infection, 200 plaque-forming unit (pfu)/cell. *(Center)* Representative images of Matrigel invasion in GBM cell lines T98G and U87. Decreases in MDA-9/syntenin expression correspond with inhibition of invasion. *(Right)* Invasion quantified using 5 fields per triplicate well. (B) Overexpression of MDA-9/syntenin leads to increases in invasion. *(Left)* Protein expression of MDA-9/syntenin after viral infection, 100 pfu/cell. *(Center)* Representative images of Matrigel invasion in IM-PHFA, Sw1783, and GBM5 lines. Increases in MDA-9/syntenin expression leads to enhanced invasion. *(Right)* Invasion quantified using 5 fields per triplicate well. ** $P < .01$.

GBM5 cells. In this experiment, the enhanced invasion we observed when overexpressing MDA-9/syntenin was mitigated when coexpressing the dominant negative c-Src protein (Fig. 3B, Supplementary Fig. 6A).

To further investigate the activation of NF-κB following forced MDA-9/syntenin expression, we transfected Sw1783 cells with a plasmid producing luciferase under the control of a promoter with NF-κB binding sites. Consequently, we expected increased luminescence in cells subsequently treated with Ad.5/3–*mda-9* compared with those treated with Ad.5/3-*vec*. As anticipated, examining cells with the reporter plasmid that overexpressed *mda-9*/syntenin, we observed a >2.5-fold induction of NF-κB activity compared with vector-infected cells (Fig. 3C).

Finally, we employed pharmacological inhibitors in vitro to confirm the pathway through which *mda-9*/syntenin exerts its effects. Using IM-PHFA and Sw1783 cell lines, cultures were infected with an Ad.5/3-*vec* or Ad.5/3–*mda-9*. These cells were then treated with dimethyl sulfoxide, IKK inhibitor, or SB203580, a p38MAPK inhibitor, and subsequently analyzed for invasive potential. As expected, overexpression of *mda-9*/syntenin leads to significant increases in invasion compared with vector-treated cells (Fig. 3D, Supplementary Figs. 6B and C). We would expect that if MDA-9/syntenin performed its invasion signaling through a pathway outside of the p38MAPK–NF-κB axis, pharmacological inhibition of these proteins would have minimal effect. Notably, both the IKK inhibitor and SB203580 abrogated the invasion gains in cells overexpressing *mda-9*/syntenin.

GBM Cells Expressing shmda-9 Show Marked Reductions in Invasion, Tumorigenesis, and Angiogenesis

To further explore the effects of *mda-9*/syntenin knockdown, clones that stably express sh*mda*-9 were produced in GBM6 cells, with substantial knockdown achieved in several of the isolated colonies (Fig. 4A). Compared with the normally invasive control clones, GBM6–sh*mda-9* clones exhibited 2.5- to 4-fold decreases in invasive ability (Fig. 4B).

The invasive capacity of GBM cells depends on both digestion of ECM, as monitored by Matrigel invasion assays, and the locomotive ability of these cells once a path is cleared. Thus, the migration rates

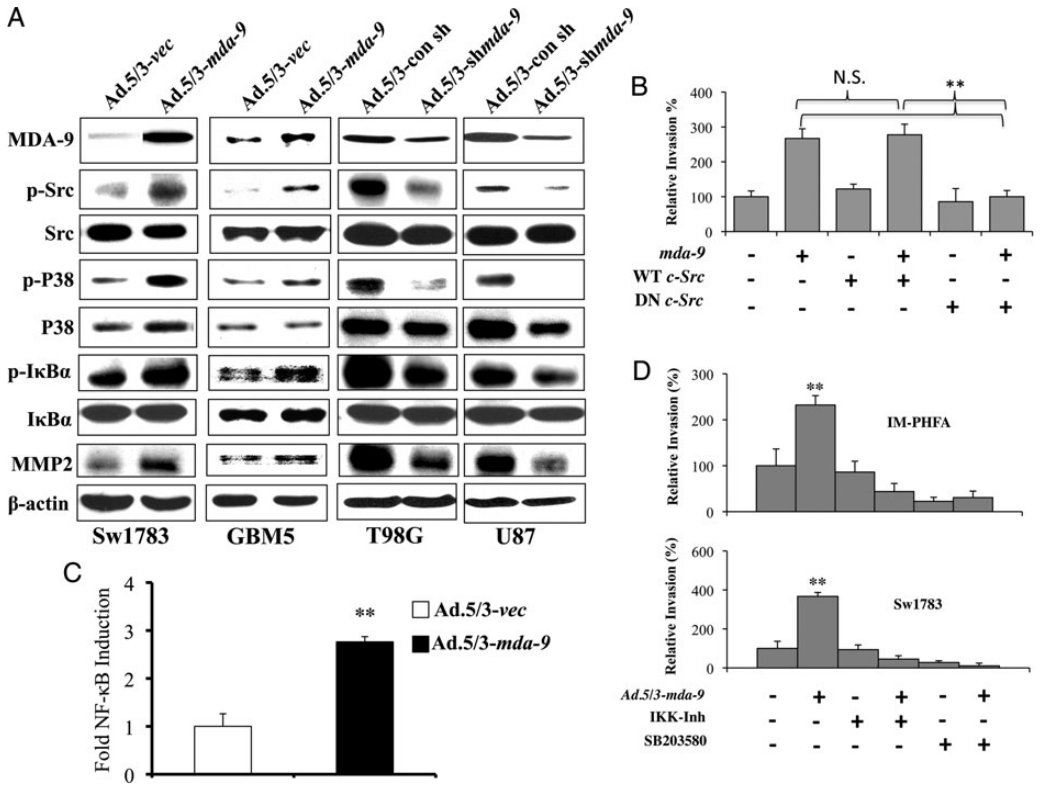

Fig. 3. MDA-9/syntenin activates NF-κB through an Src, P38MAPK-dependent pathway. (A) Protein expression following overexpression *(left columns)* or knockdown *(right columns)* in the indicated cell lines. β-actin is used as an internal control for protein loading. (B) Results from Matrigel invasion in GBM5 cells following Ad.5.3-*vec* or Ad.5/3 – *mda-9* infection and transfection with vector, wild-type Src (WT), or dominant negative (DN) dead kinase Src. Invasion quantified using 5 fields per triplicate well. (C) Fold NF-κB induction in Sw1783 cells after MDA-9/syntenin overexpression compared with vector control. NF-κB induction measured using 3κB-Luc transfection, a plasmid containing 3 tandem NF-κB binding sites upstream of the luciferase gene. (D) Results from Matrigel invasion in IM-PHFA and Sw1783 cells following Ad.5.3-*vec* or Ad.5/3 – *mda-9* infection and treatment with dimethyl sulfoxide, IKK inhibitor, or SB203580 (P38MAPK inhibitor). Invasion quantified using 5 fields per triplicate well. ** $P < .01$.

of GBM6 – sh*mda*-9 clones were analyzed by quantifying gap closure after 18 and 24 h. As a result of reduced MDA-9/syntenin levels, gap closure was reduced by as much as 50% in GBM – sh*mda*-9 cells compared with GBM6-control (Fig. 4C).

Anchorage-independent growth is an established marker for transformation and a tumorigenic phenotype in specific cancer cell types. To determine the effect of MDA-9/syntenin knockdown on the ability of transformed cells to grow in an anchorage-independent environment, GBM6-control and sh*mda-9* clones were seeded in a soft agar transformation assay (Cell Biolabs). Control GBM6 cells readily formed large and numerous colonies after 8 days of growth in soft agar. Reduced levels of MDA-9/syntenin in GBM6 – sh*mda-9* cells led to a decrease in the number and size of the colonies formed (Fig. 4D). Consequently, MDA-9/syntenin has a significant effect on the ability of transformed GBM cells to grow in an anchorage-independent environment in vitro.

Tumorigenic capacity in vivo was then analyzed by injecting 10^5 GBM6-control or GBM6 – sh*mda-9* cells subcutaneously into athymic nude mice. Tumors were measured 3 times weekly, and after 21 days the mice were sacrificed and the tumors resected and weighed. GBM6-control cells formed consistently larger tumors by volume and weight compared with their MDA-9/syntenin-depleted counterparts (Fig. 5A). Because GBM6 – sh*mda-9* clones show no differences in proliferation rate in vitro (Supplementary Fig. 7), differences in tumor size could be due to changes in angiogenic ability caused by the knockdown of MDA-9/syntenin. To test this hypothesis, we knocked down MDA-9/syntenin by Ad.5/3 – sh*mda-9* viral infection of T98G GBM cells and harvested conditioned media. By means of a CAM assay, we observed marked differences in blood vessel development when exposed to control GBM conditioned media (T98G cells infected with Ad.5/3-*vec*) compared with media from Ad.5/3 – sh*mda-9* infected T98G cells. Less microvessel development and fewer branch points were evident in membranes exposed to media from knockdown cells (Fig. 5B). Upon analysis using an angiogenic protein array, substantial reductions in the levels of secreted interleukin (IL)-8 were observed (Fig. 5C). These data are corroborated by similar trends in mRNA levels of IL-8 in T98G cells, as well as increased mRNA levels in IM-PHFA cells overexpressing MDA-9/syntenin (Fig. 5D). Moreover, secreted IL-8 levels were increased in the conditioned media of IM-PHFA cells infected with Ad.5/3 – *mda*-9 as measured by ELISA. Likewise, decreased IL-8 was detected from MDA-9/syntenin-depleted T98G cells (Fig. 5E). In total, these in vitro and in vivo data demonstrate the crucial role that MDA-9/syntenin plays in tumor formation and angiogenesis.

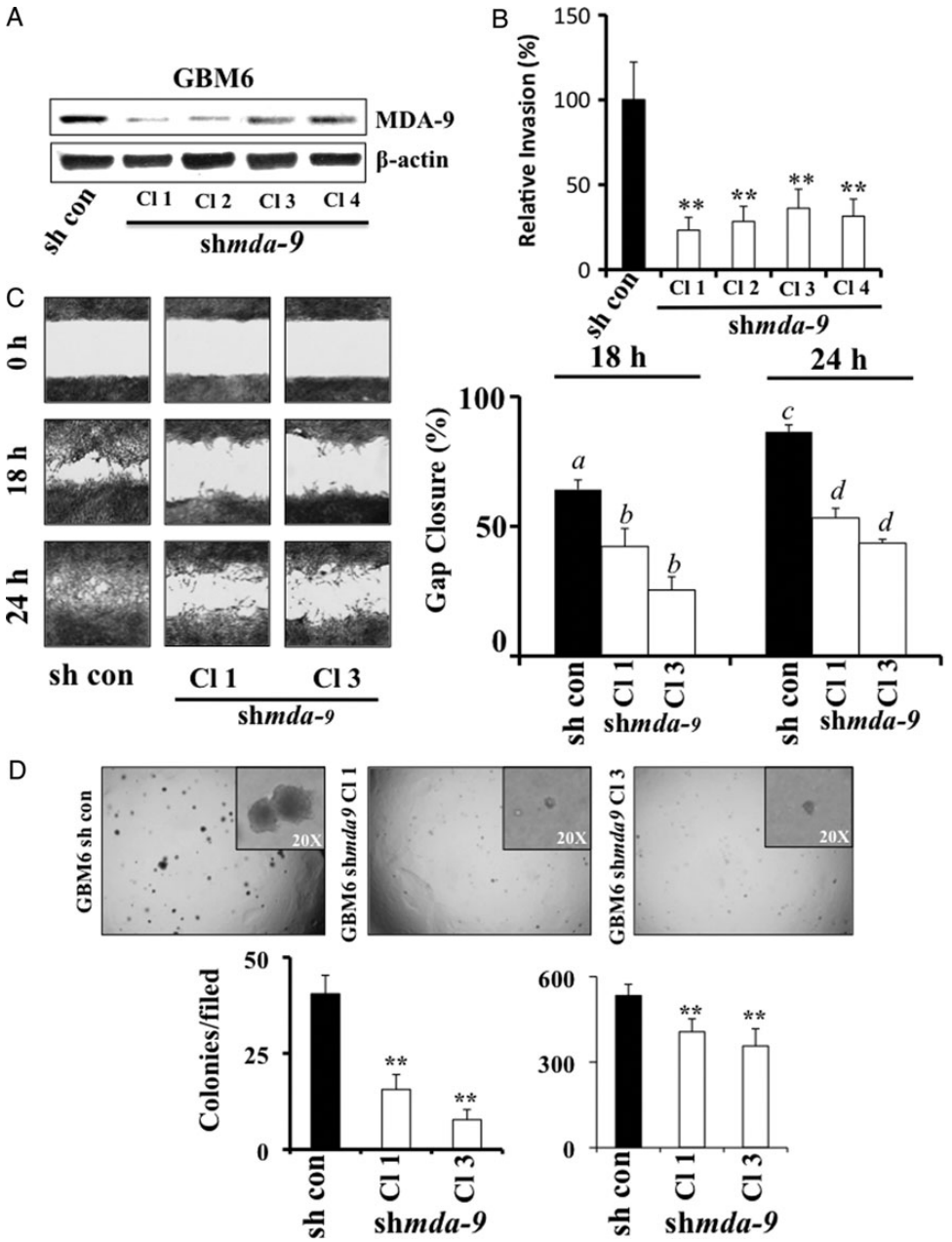

Fig. 4. Stable MDA-9/syntenin knockdown in GBM results in decreased invasion, migration, and anchorage-independent growth. (A) MDA-9/syntenin protein levels were decreased by stable expression of sh*mda-9* in GBM6 cells. (B) Results from Matrigel invasion of GBM6–sh*mda-9* clones. Invasion quantified using 5 fields per triplicate well. (C) *(Left)* Wound healing assay after 18 and 24 h in control and sh*mda-9* GBM6 Cl 1 and Cl 3. *(Right)* Quantification of triplicate wound healing scratch assays as quantified using ImageJ. *a* differs from *b* ($P < .01$), and *c* differs from *d* ($P < .01$). (D) *(Upper)* Representative images of anchorage-independent growth in soft agar using GMB6-control and sh*mda-9* clones. *(Inset)* Higher magnification illustrating the differences in colony size. *(Lower)* Quantification of colony number (left) and size (right) using ImageJ. ** $P < .01$.

Knockdown of MDA-9/syntenin Leads to Changes in Tumor Properties in an Orthotopic Tumor Model of Glioma

To provide a more authentic tumor microenvironment and to further explore the role of MDA-9/syntenin in invasion, we employed an orthotopic xenograft model in which 15 000 cells were stereotactically injected intracranially into athymic nude mice. The mice were monitored for neurological symptoms such as paralysis, seizures, weight loss, and lethargy and were sacrificed according to a protocol approved by the Institutional Animal Care and Use Committee. The survival times for the GBM6–sh*mda-9* group were significantly longer compared with the GBM6-control group by chi-square analysis ($P = .015$; Fig. 6A). Postmortem, brain and tumor tissue were collected and sectioned for immunohistochemical staining. GBM6–sh*mda-9* tumors retained a lower level of MDA-9/syntenin expression, although both control

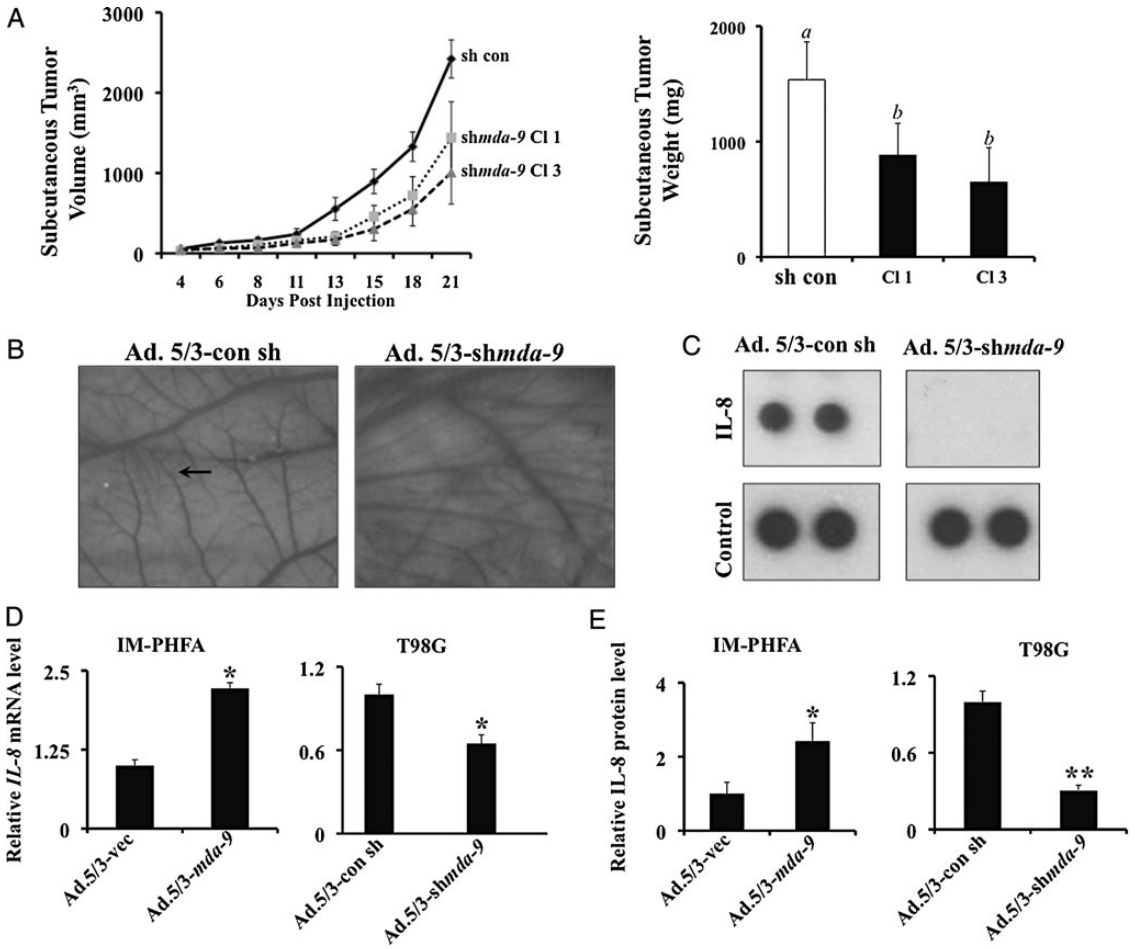

Fig. 5. MDA-9/syntenin knockdown decreases tumor size in vivo and angiogenesis in vitro. (A) *(Left)* Tumor volume from subcutaneous injection of GBM6 control and sh*mda-9* expressing clones. *(Right)* Weight of resected subcutaneous tumors after 21 days. *a* differs from *b* ($P < .01$) (B) Representative images from CAM assay using T98G cells treated with vector or Ad.5/3 – sh*mda-9*. The proliferation of the smallest vessels *(arrow)* is decreased with knockdown of MDA-9/syntenin. (C) IL-8 expression in conditioned media from treated T98G cells as measured by angiogenesis protein array. (D) Real-time PCR for IL-8 mRNA using IM-PHFA and T98G lines following the indicated treatments. (E) ELISA quantification of IL-8 protein in IM-PHFA and T98G conditioned media. Media from Ad.5/3 – sh*mda-9* treated cells is normalized to Ad.5/3-con sh treated cells. * $P < .05$, ** $P < .01$.

tumors and GBM6 – sh*mda-9* tumors showed localized increases in MDA-9/syntenin at the tumor borders (Fig. 6B). Additionally, GBM6-control tumors exhibited substantially greater CD31 expression compared with GBM6 – sh*mda-9* tumors, supporting a role for MDA-9/syntenin in GBM angiogenesis (Fig. 6B). Furthermore, noteworthy differences were found in the invasion patterns of tumors formed from GBM6-control cells and tumors from GBM6 – sh*mda-9* cells. GBM6-control tumors were notable for fingerlike projections and tumor nests separate from the main body of the tumor. Additionally, control tumors displayed prominent infiltration along Virchow-Robin spaces and conspicuous leptomeningeal invasion (Fig. 6C, upper panels). Alternatively, tumors formed from GBM6 – sh*mda-9* cells had minimal focal tumor invasion into surrounding brain parenchyma, much less than that observed in control tumors, with the majority of tumor having well-demarcated margins (Fig. 6C, lower panels). This provides additional data relative to the critical role of MDA-9/syntenin in GBM invasion and points to it as a possible target to reduce infiltration of GBM cells into surrounding brain tissue.

Discussion

We presently provide definitive evidence for a role of MDA-9/syntenin in mediating astrocytoma invasion and pathogenesis. Earlier studies implicated MDA-9/syntenin in numerous cellular functions and found its expression to be particularly relevant in cancer metastasis. While systemic metastasis of astrocytoma is highly uncommon, the propensity for local invasion of the brain parenchyma leads to challenges in treatment and inevitable tumor recurrence.[3] We found MDA-9/syntenin to be overexpressed in astrocytoma with a correlation with tumor grade (Fig. 1A and B), as grade IV astrocytomas (GBM) had the highest level of MDA-9/syntenin expression. Uncovering new targets for treatment in these tumors will be particularly important, as median survival remains about 1 year despite aggressive therapy.[3] Our invasion studies indicated that MDA-9/syntenin was a significant factor in determining invasiveness and migratory capacity of astrocytoma cells, as both forced overexpression and knockdown of MDA-9/syntenin led to alterations in invasive ability. Given the involvement

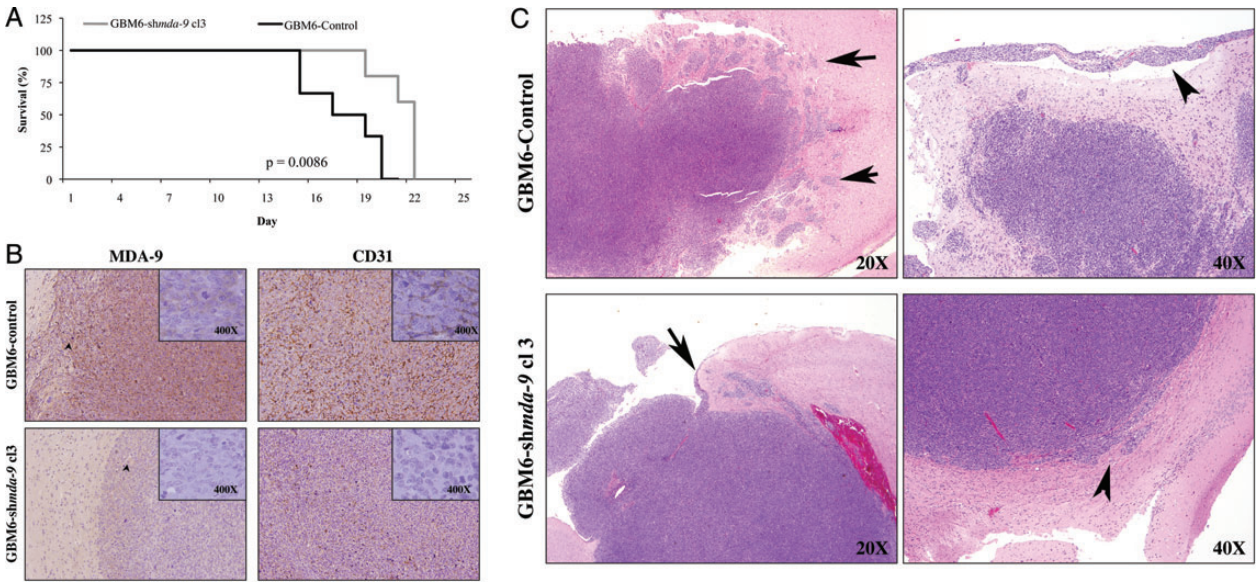

Fig. 6. MDA-9/syntenin knockdown improves survival and reduces, invasion, and angiogenesis in vivo. (A) Survival time for mice injected with GBM6-control or GBM6–sh*mda-9* Cl 3 ($P = .0086$). (B) MDA-9/syntenin and CD31 protein levels from GBM6-control tumors *(upper* and GBM–sh*mda-9* tumors *lower)*. Insert 400× magnification. (C) H&E staining from tissue collected from GBM6-control *(top row)* and GBM–sh*mda-9* tumors *(bottom row). (Upper left)* GBM6-con. Note tumor invasion surrounding brain parenchyma, with fingerlike projections and tumor nests apart from the main tumor mass showing infiltration along Virchow-Robin spaces (arrows). *(Upper right)* GBM6-con. Note leptomeningeal invasion (arrowhead). *(Lower left)* GBM6–sh*mda-9*. Very focal leptomeningeal invasion compared with control (arrow). *(Lower right)* GBM6–sh*mda-9*. Minimal focal tumor invasion into surrounding brain parenchyma (arrowhead) with a largely demarcated margin.

of MDA-9/syntenin in crucial early stages of development in the CNS, this suggests that MDA-9/syntenin may be an important genetic component in less differentiated precursor cells, with which glioma cells share remarkable similarities, notably the ability of single cells to migrate throughout the brain.[31]

An essential aspect of tumor migration and invasion is the interaction of single cells with the ECM. Vital contributors in these interactions include one of the most important groups of adhesion molecules in glioma migration and invasion, the integrins, which act as signal mediators and anchors to the ECM.[32] Specifically, high expression of the integrin β1 subunit correlates with invasive behavior in glioma.[33] Immunoprecipitation of β1 integrin in melanoma and breast cancer revealed that fibronectin interactions increased FAK–c-Src–MDA-9/syntenin signaling complexes, shown to be important regulators of the migration and invasion machinery.[34,35] We document that in astrocytoma, MDA-9/syntenin expression leads to c-Src activation and downstream effects on the p38MAPK pathway, resulting in enhanced invasion. Furthermore, MDA-9/syntenin has been linked to a key mediator of integrin and signaling of phosphatidylinositol-3 kinase (PI3K): integrin linked kinase (ILK).[34] ILK is a serine/threonine kinase that acts as a molecular tether point, can regulate protein-protein interactions, and coordinates the organization of the actin cytoskeleton.[36] Conspicuously, phosphatase and tensin homolog, inactivated in a large percentage of high-grade astrocytomas,[37] can inhibit the activity of ILK in addition to PI3K.[38,39]

NF-κB is activated through overexpression of MDA-9/syntenin, and conversely it can be inhibited through knockdown of MDA-9/syntenin. Syndecan-1, a member of a major group of cell surface proteoglycans, is overexpressed in GBM samples and may be regulated by NF-κB.[40] This serves as another possible link between MDA-9/syntenin and glioma, as one of the earlier observations of MDA-9/syntenin came through its identification as binding the cytoplasmic domain of syndecans.[9] Additionally, pharmacological inhibition of downstream c-Src effectors abrogates the invasion gains accrued through MDA-9/syntenin overexpression. Upstream, c-Src has been linked to an important and common alteration found in GBM, the amplification or mutation of epidermal growth factor receptor (EGFR), giving credence to the possibility of MDA-9/syntenin playing a role in this important signaling pathway.[41–44] Moreover, in a recent study, a physical interaction and colocalization of MDA-9/syntenin and EGFR was evident in human urothelial cell carcinoma cell lines and primary tumors.[45]

While anti-angiogenic therapy currently exists for high-grade astrocytoma, these tumors have been shown to evade cell death through hypoxia-induced autophagy, adapting to therapy through induction of hypoxia-inducible factor (HIF)–1α.[46] MDA-9/syntenin induction leads to HIF-1α expression in human melanoma (data not shown). IL-8 has proven to be a particularly important cytokine in glioma biology. Mutant EGFR signaling acts through NF-κB to induce secretion of IL-8, leading to an enhanced xenograft neovascularization.[47] Additionally, IL-8 is a mediator of invasion in gliomas, also acting through the NF-κB pathway.[48] The angiogenic effect of MDA-9/syntenin in glioma deserves further exploration, as another recent study implicated the syndecan–MDA-9/syntenin–Alix axis in the biogenesis of exosomes, which can be secreted from tumor cells and contain mRNA and proteins.[49] In GBM, exosomes have been shown to contain translatable mRNA and can contribute to growth and angiogenesis. In addition to the clinical importance of MDA-9/syntenin in patient survival demonstrated in Fig. 1C, mining the National Cancer Institute's Repository of Molecular Brain Neoplasia Data database corroborated this finding in human glioma

patients. In GBM patients with *mda-9*/syntenin upregulated >2.0×, survival was significantly shorter ($P = .0016$). Furthermore, in all glioma patients with *mda-9*/syntenin upregulated >2.0×, survival was again significantly reduced ($P = 6.0 \times 10^{-5}$).[50]

Through our in vivo studies, we demonstrate that MDA-9/syntenin is a major contributor to the deadliest aspect of GBM pathology, invasion. Combined with our analysis of patient samples and in vitro data, we propose that MDA-9/syntenin could prove to be a valuable target for the treatment of high-grade glioma.

Supplementary Material

Supplementary material is available online at *Neuro-Oncology* (http://neuro-oncology.oxfordjournals.org/).

Funding

The present study was supported in part by the National Institutes of Health, NCI grants R01 CA097318 and R01 CA134721 to P.B.F.; and a James S. McDonnell Foundation 21st Century Science Initiative Grant to D.S.

Acknowledgments

D.S. is a Harrison Scholar in the VCU Massey Cancer Center. P.B.F. holds the Thelma Newmeyer Corman Chair in Cancer Research in the VCU Massey Cancer Center.

Conflict of interest statement. None declared.

References

1. *CBTRUS Statistical Report: Primary Brain and Central Nervous System Tumors Diagnosed in the United States in 2004–2008*. Hinsdale, IL: Central Brain Tumor Registry of the United States; 2012.
2. Kleihues P, Louis DN, Scheithauer BW, et al. The WHO classification of tumors of the nervous system. *J Neuropathol Exp Neurol*. 2002;61(3): 215–225; discussion 226–219.
3. Nakada M, Nakada S, Demuth T, Tran NL, Hoelzinger DB, Berens ME. Molecular targets of glioma invasion. *Cell Mol Life Sci*. 2007;64(4): 458–478.
4. Onishi M, Ichikawa T, Kurozumi K, Date I. Angiogenesis and invasion in glioma. *Brain Tumor Pathol*. 2011;28(1):13–24.
5. Burger PC, Heinz ER, Shibata T, Kleihues P. Topographic anatomy and CT correlations in the untreated glioblastoma multiforme. *J Neurosurg*. 1988;68(5):698–704.
6. Westphal M, Lamszus K. The neurobiology of gliomas: from cell biology to the development of therapeutic approaches. *Nat Rev Neurosci*. 2011; 12(9):495–508.
7. Beadle C, Assanah MC, Monzo P, Vallee R, Rosenfeld SS, Canoll P. The role of myosin II in glioma invasion of the brain. *Mol Biol Cell*. 2008;19(8): 3357–3368.
8. Lin JJ, Jiang HP, Fisher PB. Characterization of a novel melanoma differentiation-associated gene, mda-9, that is down-regulated during terminal cell differentiation. *Mol Cell Differ*. 1996;4(4):317–333.
9. Grootjans JJ, Zimmermann P, Reekmans G, et al. Syntenin, a PDZ protein that binds syndecan cytoplasmic domains. *Proc Natl Acad Sci U S A*. 1997;94(25):13683–13688.
10. Sarkar D, Boukerche H, Su ZZ, Fisher PB. Mda-9/syntenin: more than just a simple adapter protein when it comes to cancer metastasis. *Cancer Research*. 2008;68(9):3087–3093.
11. Sarkar D, Boukerche H, Su ZZ, Fisher PB. Mda-9/syntenin: recent insights into a novel cell signaling and metastasis-associated gene. *Pharmacol Ther*. 2004;104(2):101–115.
12. Das SK, Bhutia SK, Kegelman TP, et al. MDA-9/syntenin: a positive gatekeeper of melanoma metastasis. *Front Biosci*. 2012;17:1–15.
13. Beekman JM, Coffer PJ. The ins and outs of syntenin, a multifunctional intracellular adaptor protein. *J Cell Sci*. 2008;121(Pt 9):1349–1355.
14. Lin JJ, Jiang H, Fisher PB. Melanoma differentiation associated gene-9, mda-9, is a human gamma interferon responsive gene. *Gene*. 1998; 207(2):105–110.
15. Boukerche H, Su ZZ, Emdad L, Sarkar D, Fisher PB. Mda-9/syntenin regulates the metastatic phenotype in human melanoma cells by activating nuclear factor-kappaB. *Cancer Res*. 2007;67(4):1812–1822.
16. Boukerche H, Su ZZ, Prevot C, Sarkar D, Fisher PB. Mda-9/syntenin promotes metastasis in human melanoma cells by activating c-Src. *Proc Natl Acad Sci USA*. 2008;105(41):15914–15919.
17. Boukerche H, Su ZZ, Emdad L, et al. Mda-9/syntenin: a positive regulator of melanoma metastasis. *Cancer Res*. 2005;65(23):10901–10911.
18. Boukerche H, Aissaoui H, Prevost C, et al. Src kinase activation is mandatory for MDA-9/syntenin-mediated activation of nuclear factor-kappaB. *Oncogene*. 2010;29(21):3054–3066.
19. Koo TH, Lee JJ, Kim EM, Kim KW, Kim HD, Lee JH. Syntenin is overexpressed and promotes cell migration in metastatic human breast and gastric cancer cell lines. *Oncogene*. 2002;21(26): 4080–4088.
20. Zhong D, Ran JH, Tang WY, et al. Mda-9/syntenin promotes human brain glioma migration through focal adhesion kinase (FAK)-JNK and FAK-AKT signaling. *Asian Pac J Cancer Prev*. 2012;13(6):2897–2901.
21. Lambaerts K, Van Dyck S, Mortier E, et al. Syntenin, a syndecan adaptor and an Arf6 phosphatidylinositol 4,5-bisphosphate effector, is essential for epiboly and gastrulation cell movements in zebrafish. *J Cell Sci*. 2012;125(Pt 5):1129–1140.
22. Tomoda T, Kim JH, Zhan C, Hatten ME. Role of Unc51.1 and its binding partners in CNS axon outgrowth. *Genes Dev*. 2004;18(5):541–558.
23. Dash R, Dmitriev I, Su ZZ, et al. Enhanced delivery of mda-7/IL-24 using a serotype chimeric adenovirus (Ad.5/3) improves therapeutic efficacy in low CAR prostate cancer cells. *Cancer Gene Therapy*. 2010;17(7): 447–456.
24. Mittereder N, March KL, Trapnell BC. Evaluation of the concentration and bioactivity of adenovirus vectors for gene therapy. *J Virol*. 1996; 70(11):7498–7509.
25. Yacoub A, Hamed H, Emdad L, et al. MDA-7/IL-24 plus radiation enhance survival in animals with intracranial primary human GBM tumors. *Cancer Biol Ther*. 2008;7(6):917–933.
26. Su ZZ, Leszczyniecka M, Kang DC, et al. Insights into glutamate transport regulation in human astrocytes: cloning of the promoter for excitatory amino acid transporter 2 (EAAT2). *Proc Natl Acad Sci U S A*. 2003;100(4):1955–1960.
27. Emdad L, Lee SG, Su ZZ, et al. Astrocyte elevated gene-1 (AEG-1) functions as an oncogene and regulates angiogenesis. *Proc Natl Acad Sci U S A*. 2009;106(50):21300–21305.
28. Pfeifer A, Kessler T, Silletti S, Cheresh DA, Verma IM. Suppression of angiogenesis by lentiviral delivery of PEX, a noncatalytic fragment of matrix metalloproteinase 2. *Proc Natl Acad Sci U S A*. 2000;97(22): 12227–12232.

29. Sun L, Hui A-M, Su Q, et al. Neuronal and glioma-derived stem cell factor induces angiogenesis within the brain. *Cancer Cell*. 2006;9(4): 287–300.
30. Goldman M, Craft B, Swatloski T, et al. The UCSC Cancer Genomics Browser: update 2013. *Nucleic Acids Res*. 2013;41(Database issue): D949–D954.
31. Cayre M, Canoll P, Goldman JE. Cell migration in the normal and pathological postnatal mammalian brain. *Prog Neurobiol*. 2009; 88(1):41–63.
32. Hemler ME. Integrin associated proteins. *Curr Opin Cell Biol*. 1998;10(5): 578–585.
33. Paulus W, Baur I, Beutler AS, Reeves SA. Diffuse brain invasion of glioma cells requires beta 1 integrins. *Lab Invest*. 1996;75(6):819–826.
34. Hwangbo C, Kim J, Lee JJ, Lee JH. Activation of the integrin effector kinase focal adhesion kinase in cancer cells is regulated by crosstalk between protein kinase Calpha and the PDZ adapter protein mda-9/ syntenin. *Cancer Res*. 2010;70(4):1645–1655.
35. Schlaepfer DD, Mitra SK. Multiple connections link FAK to cell motility and invasion. *Curr Opin Genet Dev*. 2004;14(1):92–101.
36. D'Abaco GM, Kaye AH. Integrin-linked kinase: a potential therapeutic target for the treatment of glioma. *J Clin Neurosci*. 2008;15(10): 1079–1084.
37. Engelman JA, Luo J, Cantley LC. The evolution of phosphatidylinositol 3-kinases as regulators of growth and metabolism. *Nat Rev Genet*. 2006;7(8):606–619.
38. Delcommenne M, Tan C, Gray V, Rue L, Woodgett J, Dedhar S. Phosphoinositide-3-OH kinase-dependent regulation of glycogen synthase kinase 3 and protein kinase B/AKT by the integrin-linked kinase. *Proc Natl Acad Sci U S A*. 1998;95(19):11211–11216.
39. Morimoto AM, Tomlinson MG, Nakatani K, Bolen JB, Roth RA, Herbst R. The MMAC1 tumor suppressor phosphatase inhibits phospholipase C and integrin-linked kinase activity. *Oncogene*. 2000;19(2):200–209.
40. Watanabe A, Mabuchi T, Satoh E, et al. Expression of syndecans, a heparan sulfate proteoglycan, in malignant gliomas: participation of nuclear factor-kappaB in upregulation of syndecan-1 expression. *J Neurooncol*. 2006;77(1):25–32.
41. Paugh BS, Paugh SW, Bryan L, et al. EGF regulates plasminogen activator inhibitor-1 (PAI-1) by a pathway involving c-Src, PKCdelta, and sphingosine kinase 1 in glioblastoma cells. *FASEB J*. 2008;22(2): 455–465.
42. Lu KV, Zhu S, Cvrljevic A, et al. Fyn and SRC are effectors of oncogenic epidermal growth factor receptor signaling in glioblastoma patients. *Cancer Res*. 2009;69(17):6889–6898.
43. Yang M, Li Y, Chilukuri K, et al. L1 stimulation of human glioma cell motility correlates with FAK activation. *J Neurooncol*. 2011; 105(1):27–44.
44. Feng H, Hu B, Jarzynka MJ, et al. Phosphorylation of dedicator of cytokinesis 1 (Dock180) at tyrosine residue Y722 by Src family kinases mediates EGFRvIII-driven glioblastoma tumorigenesis. *Proc Natl Acad Sci U S A*. 2012;109(8):3018–3023.
45. Dasgupta S, Menezes M, Das SK, et al. Novel role of MDA-9/syntenin in regulating urothelial cell proliferation by modulating EGFR signaling. *Clin Cancer Res*. 2013;19(17):4621–4633.
46. Hu YL, DeLay M, Jahangiri A, et al. Hypoxia-induced autophagy promotes tumor cell survival and adaptation to antiangiogenic treatment in glioblastoma. *Cancer Res*. 2012;72(7):1773–1783.
47. Bonavia R, Inda MM, Vandenberg S, et al. EGFRvIII promotes glioma angiogenesis and growth through the NF-kappaB, interleukin-8 pathway. *Oncogene*. 2012;31(36):4054–4066.
48. Raychaudhuri B, Vogelbaum MA. IL-8 is a mediator of NF-kappaB induced invasion by gliomas. *J Neurooncol*. 2011;101(2):227–235.
49. Baietti MF, Zhang Z, Mortier E, et al. Syndecan-syntenin-ALIX regulates the biogenesis of exosomes. *Nat Cell Biol*. 2012;14(7):677–685.
50. National Cancer Institute. 2005. REMBRANDT home page. http:// rembrandt.nci.nih.gov. Accessed 2012.